BioChip Journal (2022) 16:197–206
https://doi.org/10.1007/s13206-022-00058-z

ORIGINAL ARTICLE

Detection and Real-Time Monitoring of LDL-Cholesterol by Redox-Free Impedimetric Biosensors

Abdulaziz K. Assaifan[1] · Fatimah A. Alqahtani[1] · Sarah Alnamlah[2] · Rasha Almutairi[1] · Hend I. Alkhammash[3]

Received: 26 January 2022 / Revised: 27 March 2022 / Accepted: 12 April 2022 / Published online: 6 May 2022

Abstract
In this work, non-faradaic impedimetric biosensor was developed for the direct detection of low-density lipoprotein (LDL-cholesterol). Unlike other electrochemical techniques, non-faradaic electrochemical impedance spectroscopy (EIS) does not require the use of redox probes which denatures targeted biomarkers. Furthermore, no reference electrode is required for detection which is commercially viable. The biosensor reported here consists of LDL-antibodies attached to interdigitated gold electrodes via standard chemical functionalization. The biosensor demonstrated a sensitivity and limit of detection (LoD) of 70 nF/log(ng/mL) and 120 pg/mL, respectively, where the LoD is well below the recommended LDL level in blood. The biosensor also demonstrated good selectivity toward LDL. Thereafter we utilized, for the first time, the non-faradaic impedimetric biosensor for the continuous monitoring of LDL in phosphate buffer saline (PBS). The biosensor showed rapid responses to LDL injections. Such an approach is essential for the development of low-cost and scalable wearable biosensors for the direct real-time monitoring of chronic diseases and hence allows early medical interventions in cases where sudden increases in LDL or other biomarkers are deadly.

Keywords Chronic diseases · LDL detection · Non-faradaic · Real-time monitoring

1 Introduction

Cholesterol is an important source of bioactive molecules such as steroid hormones, vitamin D and bile acids, which can regulate cellular metabolism and both intracellular and extracellular communication [1]. Furthermore, the human body requires cholesterol to build the structure of cell membranes for the nervous system, peripheral nerves and the brain [1]. There are five major groups of lipoproteins responsible for the transport of different fat molecules such as cholesterol around the body where it is demanded [2, 3]. Out of these major groups, low-density lipoprotein (LDL) which is composed of 75–80% lipid and 20–25% apolipoprotein B-100 (apo B-100), can be recognized by specific receptors on cells' surfaces. During cholesterol transport, apo B-100 of LDL can interact with sulphated glycosaminoglycans resulting in the accumulation of cholesterol at the arterial walls leading to plaque formation and eventually blood clotting [4]. Therefore, excessive amounts of LDL cholesterol in the bloodstream may eventually lead to vascular diseases [5]. Hence, LDL is sometimes referred to as "bad cholesterol". According to the National Cholesterol Education Program (NCEP, USA), optimal LDL and total cholesterol concentrations are < 1000 mg/L and < 2000 mg/L, respectively [3, 6]. In this regard, accurate quantification of LDL is important. There are multiple conventional analytical methods which have been used for the analysis of LDL, such as ultracentrifugation and NMR spectroscopy. However, for general clinical use, these methods are tedious and time-consuming. Therefore, label free, direct and simple detection techniques of high LDL levels is essential.

Biosensors are more promising for the direct and easy detection of LDL without complicated steps. Researchers have attempted the detection of LDL using sensors based on quartz crystal microbalance (QCM) [7], optical [8, 9], enzymatic [10], fluorescence [11] and electrochemical biosensors

✉ Abdulaziz K. Assaifan
aassaifan@ksu.edu.sa

[1] King Abdullah Institute for Nanotechnology, King Saud University, PO Box 2455, Riyadh 11451, Saudi Arabia

[2] College of Dentistry, King Saud University, PO Box 60169, Riyadh 11545, Saudi Arabia

[3] Department of Electrical Engineering, College of Engineering, Taif University, PO Box 11099, Taif 21944, Saudi Arabia

[12]. Despite the sensitivity of the abovementioned techniques, they can be bulky, tedious, time consuming and require highly trained individuals.

Electrochemical biosensors have gained a lot of interest due to their low cost, ease-of-use and label-free detection. In addition, they are not composed of bulky components like the other transduction techniques, hence facilitating the production of portable devices for the monitoring of chronic diseases in the future. However, for LDL detection, the majority of reported electrochemical techniques are based on cyclic voltammetry (CV) [13], square-wave voltammetry (SWV) [14] and faradaic impedimetric detection which require the use of redox probes and/or reference electrodes during detection. Therefore, there is still limitations regarding the use of miniaturized and simple electrochemical biosensors for label-free and direct LDL detection. Non-faradaic impedimetric biosensors are an emerging electrochemical detection technique. Unlike other electrochemical biosensors which rely on oxidation/reduction reactions, non-faradaic sensors do not require the use of redox probes, nor the involvement of reference electrodes during detection, hence, even simpler and lower-in cost LDL detection. The use of a non-faradaic technique avoids biomolecules denaturation since no redox probe is used. The commonly used redox probe (Ferro/Ferricyanide $[Fe(CN)6]^{3-/4-}$) can denature biomolecules due to its toxic nature [15]. Furthermore, the use of a redox probe would add an additional step to LDL detection and hence non-faradaic sensors can be more suitable for point-of-care diagnostics. Additionally, non-faradaic sensors are operated at small AC voltages which preserve the biomolecular layers at the electrode/electrolyte interface. conductive electrodes for non-faradaic biosensing are usually fabricated on top of the flexible plastic substrate which allows them to be worn on the skin and integrated more easily with sampling platforms. In addition, the ability to perform biosensing without reference electrodes encourages the miniaturization of electronics at low-cost. The technique is based on capacitive changes at the electrode/electrolyte interface. Upon receptor/biomarker interaction, the interfacial capacitance is altered due to changes in the charges, area, thickness or dielectric at the biosensor surface [16, 17]. Non-faradaic biosensors are very promising for the rapid and direct detection of diseases where any individual can use them. The technique has been recently used for the direct detection of viruses [18], water contaminants [19] and different diseases [20, 21].

Herein, we report a simple non-faradaic biosensor for the direct detection of LDL cholesterol. The biosensor consists of interdigitated gold electrodes functionalized with cysteamine and glutaraldehyde as the molecular linkers. Then, LDL-antibodies were attached to the surface followed by blocking with bovine serum albumin (BSA) to enhance the stability and selectivity of the biosensors. We investigated the sensitivity, LoD and selectivity of the biosensors. The biosensors showed good responses against different LDL concentrations injections and reasonable stability against blank samples. Thereafter, we introduced the utilization of non-faradaic biosensors for the continuous monitoring of LDL-cholesterol. This continuous monitoring platform is promising for monitoring patients in intensive care units or who require continuous check-up of dangerous biomarkers. It also allows clinicians to notice any changes and to see if treatments for chronic diseases are working. This approach can be implemented for other chronic diseases which require real-time monitoring.

2 Experimental Details

2.1 Materials

Interdigitated gold electrodes (Au-IDEs) on top of the plastic substrate (Fig. 1) were purchased from Metrohm-Dropsense (ref. PW-IDEAU100), Oviedo, Spain. The dimensions for bands and gaps of the Au-IDEs are 100 µm. Cysteamine, glutaraldehyde (25% in H_2O), bovine serum albumin (BSA) and ethanol absolute were procured from Sigma Aldrich,

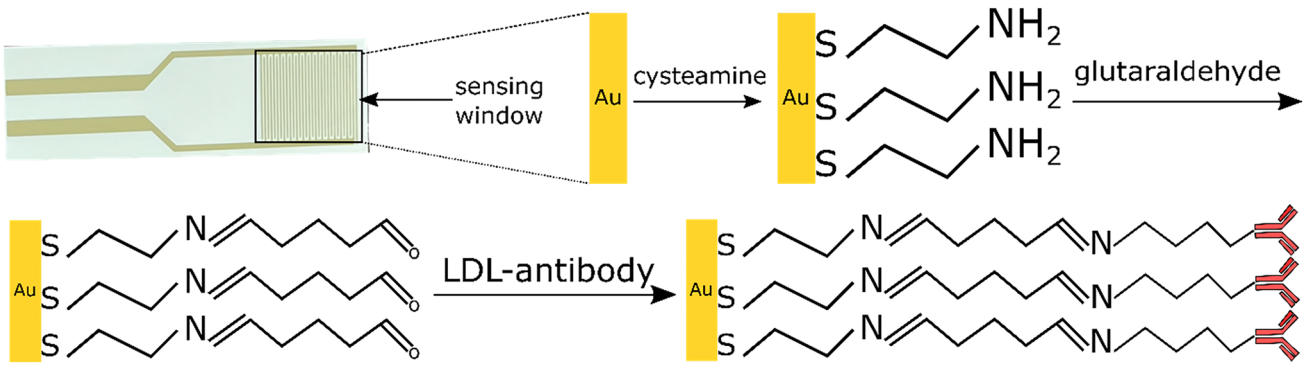

Fig. 1 Biofunctionalization of Au-IDEs with LDL-antibodies

USA. phosphate buffer silane (PBS) (pH 7.4) was supplied by Fisher Scientific, USA. LDL-antibodies and LDL-antigens were purchased from Sino Biological, China. UL83 proteins were purchased from Virusys-corporation, USA. Pepsin was obtained from SrL, India. *Escherichia coli* (*E. coli*) bacteria, which is a routine lab strain, was propagated in luria bertani (LB) media at 37 °C according to standard procedures.

2.2 Biofunctionalization

Figure 1 illustrates the biofunctionalization steps of the LDL non-faradaic biosensor. First, the sensing window of Au-IDEs was incubated with an ethanolic solution of 1 mM cysteamine for one hour in darkness at room temperature. The sensing window was then rinsed with ethanol and blown dried with nitrogen. Then, 50 µL of 2.5% glutaraldehyde in PBS was incubated in the sensing window for one hour. This was followed by rinsing with deionized water and blow-drying with nitrogen. LDL-antibodies were then attached to the surface by incubating the sensing window with 50 µL of 1 µg/mL LDL-antibody in DI water for one hour. Rinsing with deionized water was then carried out. Finally, blocking was performed by introducing 5% of 50 µL BSA in PBS for 30 min. The sensing window was then rinsed with deionized water and blown dried with nitrogen for sensor testing.

2.3 Biosensor Testing

2.3.1 Non-faradaic Biosensor Performance

Non-faradaic EIS measurements were carried out using GAMRY (interface 1000™) potentiostat. Prior to LDL detection, the baseline was measured as the following; the sensing window shown in Fig. 1 was introduced with 50 µL PBS. Before non-faradaic detection, the open circuit potential (OCP) is measured between the two electrodes to ensure that the system is at equilibrium by setting the VDC to zero with respect to OCP, it will offset the potential bias between the two electrodes. Then, OCP measurement was carried out for 100 s, followed by EIS measurements in the frequency range 200 mHz to 100 kHz with an applied sinusoidal perturbation of 10 mV. EIS measurements were repeated three times until a stable baseline was achieved. After extracting the baseline, the PBS droplet was rinsed with deionized water followed by nitrogen blow-drying. Different concentrations of LDL-antigen in PBS were then introduced onto the sensing window (from 50 pg/mL to 5 µg/mL) followed by EIS measurements. Rinsing with deionized water was performed after each LDL-antigen concentration incubation. Each concentration incubation lasted for 5 min and changes in capacitance were normalized to the baseline of the biosensor. Similar EIS measurements were performed against successive PBS (blank) incubations. These steps are important to evaluate the biosensor performance (i.e. sensitivity and limit of detection (LoD)) of the biosensor. Changes in real impedance (Z_{real}), imaginary impedance (Z_{imag}), capacitance, impedance magnitude (|Z|) and phase were normalized to the baseline of the biosensor. All experiments were repeated three times against LDL-antigen and against the blank samples. Another important factor of the biosensors is selectivity, we tested the biosensors against positive samples containing a mixture of LDL-antigen, UL83-antigen, pepsin and *E. coli*. Additionally, the biosensors were tested against negative samples which contain UL83-antigen, pepsin and *E. coli* only. UL83-antigen, pepsin and *E. coli* can be available in blood samples and may interfere in real samples testing [22–24].

2.3.2 Continuous Monitoring

EIS runs the experiments within a wide range of frequency. It takes around 3 min to run a complete EIS cycle if the frequency range is set to 200 mHz to 100 kHz. To perform EIS continuous monitoring, EIS cycle has to be limited to only a single frequency to speed up the measurement. In our work, maximum capacitive changes upon LDL-antibody/LDL-antigen binding were observed at 398 mHz. Therefore, for the continuous monitoring of LDL, we narrowed the frequency range to only 398 mHz. Measurements were performed with an applied sinusoidal perturbation of 10 mV. Firstly, the sensing window was introduced with 50 µL PBS, then EIS measurements at only 398 mHz were carried out. The next EIS cycle, 500 pg/mL of LDL was injected into the PBS droplet and EIS cycles were repeated until no significant change in capacitance was observed. Then, 5 ng/mL LDL was injected into the PBS droplet and EIS measurements were repeated until we observed no significant change in capacitance. The same procedure was repeated for LDL concentrations of 50 ng/mL, 500 ng/mL 0 and 5 µg/mL. Each EIS cycle lasted for around 15 s. Similar experiment was carried out against only PBS (blank) without injecting any molecules to observe the changes in capacitance against blank samples and to understand the behaviour of the biosensors.

3 Results and Discussion

3.1 Sensor Testing Performance

Figure 2a and b represent the Nyquist plots for the non-faradaic sensors tested against LDL-antigen and PBS (blank) samples, respectively. The large incomplete semi-circle shown in Fig. 2a and b is due to the slow electron transfer since no redox probe is used. The semi-circle shown is

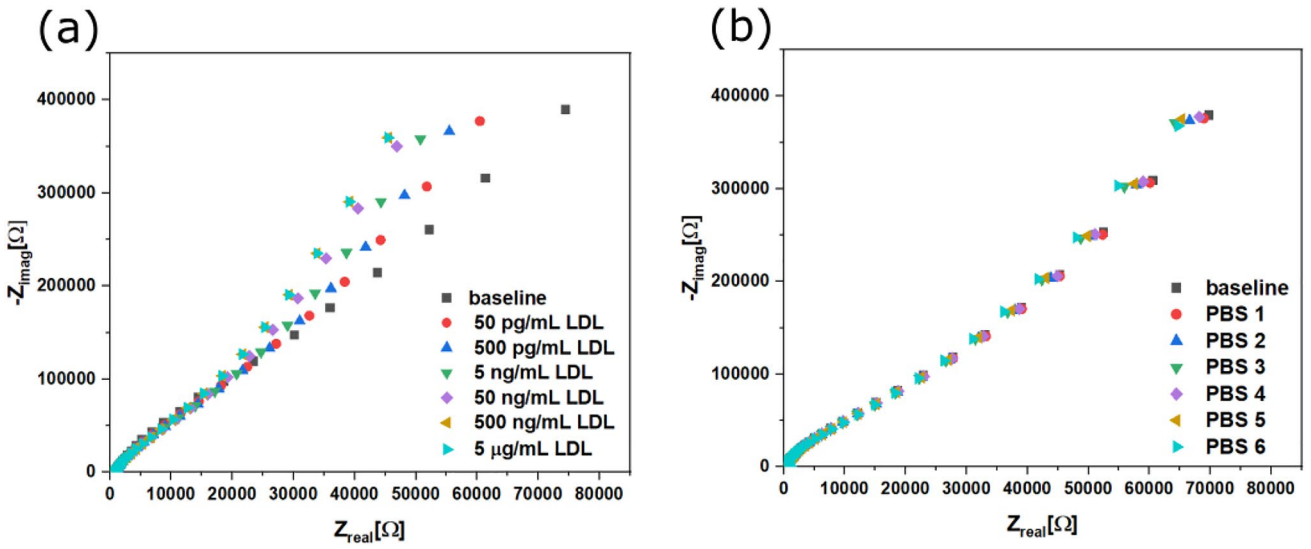

Fig. 2 Nyquist plot for **a** non-faradaic biosensor tested against different concentrations of LDL-antigen and **b** against successive PBS (blank) sample incubations

a characteristic of non-faradaic impedimetric biosensors where the charge transfer resistance and Warburg impedance (W_z) are infinite [25, 26]. Figure 2a is the Nyquist plot for the non-faradaic biosensors tested against LDL-antigen concentrations. After 6 incubations with LDL-concentrations (from 50 pg/mL to 5 µg/mL), Z_{imag} decreased from 214.4 to 190.7 kΩ at 398 mHz. Similarly, Z_{real} decreased from 43.7 kΩ (for the baseline) to 29.26 kΩ (for the largest LDL-antigen concentration). This indicates that both capacitive and resistive components are being affected. This was observed in previous literature for non-faradaic sensors using gold as electrodes [20]. Testing the biosensors against PBS samples resulted in a decrease of around 4 kΩ and 3 kΩ for Z_{imag} and Z_{real}, respectively (see Fig. 2b).

Different parameters such as capacitance, phase and impedance magnitude (|Z|) were investigated. Firstly, the change in capacitance is discussed since it showed the best limit of detection (LoD) as compared to that of phase and |Z|. Figure 3a and b show typical Bode plots for the non-faradaic biosensors against LDL-antigen and PBS (blank), respectively. Changes in capacitance were observed in a wide frequency range. However, the maximum change in capacitance was observed at 398 mHz. According to Fig. 3a, as the LDL concentration increases, the capacitance increases until it

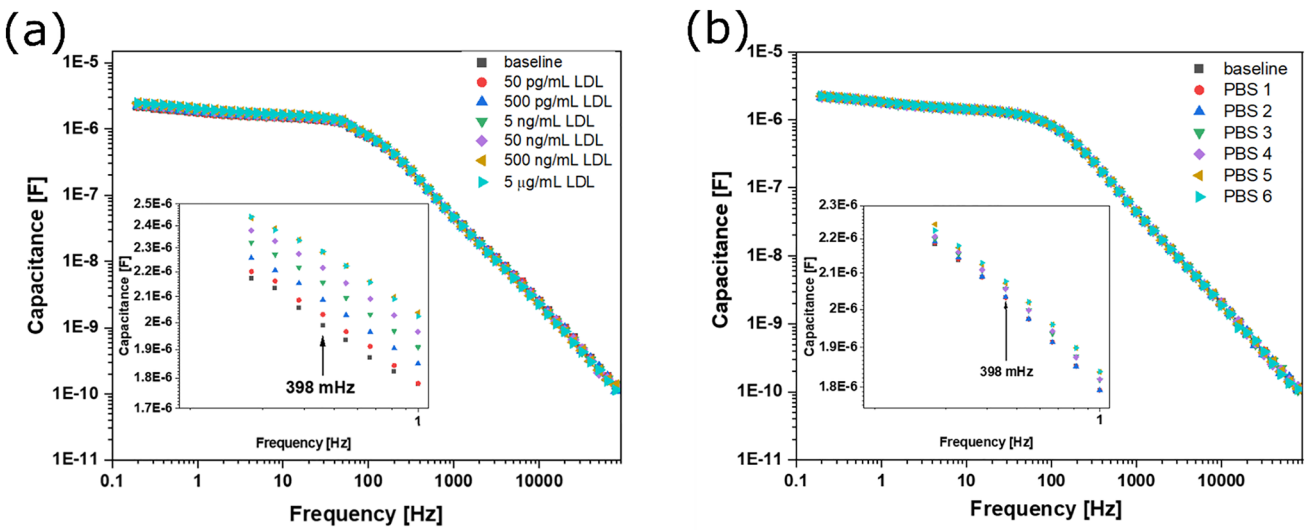

Fig. 3 Typical Bode plots representing change in capacitance for **a** non-faradaic biosensor tested against different concentrations of LDL-antigen and **b** against successive incubations of PBS (blank)

reaches saturation at 500 ng/mL LDL-antigen concentration. No significant increase in capacitance was observed against the blank sample (Fig. 3b). This illustrates that the biosensor is responding to LDL-antigen concentrations and has acceptable stability behaviour against the blank samples.

Figure 4a shows the change in capacitance at 398 mHz when biosensors were tested against LDL-antigen and blank samples. The change in capacitance increased as the LDL-antigen concentration increased from 50 pg/mL to 500 ng/mL. Further increasing the LDL concentration resulted in no capacitive changes since the biosensor saturated after incubating it with 500 ng/mL LDL. First, an average change in capacitance of around 22 nF was observed when incubating the biosensor with 50 pg/mL LDL. The biosensors demonstrated an average change in capacitance of 75 nF when incubated with 500 pg/mL LDL. Then, the average change in capacitance increased to 160 nF when sensors were incubated with 5 ng/mL LDL. The average change in capacitance as a result of incubating the biosensors with 50 ng/mL and 500 ng/mL increased to 222 nF and 285 nF, respectively. No further changes in capacitance were observed when incubating the biosensors with higher LDL concentrations due to saturation. To explain the increase in capacitance, when the conductive Au electrodes come in contact with the ionic PBS solution, an interfacial capacitance forms between the electrode/electrolyte interface. This capacitance can be altered by changes in surface roughness, permittivity, charge carried density and double layer thickness. When there are large concentrations of the antigen, there will be large molecular interaction with the antibody at the sensitive interfacial capacitance. The increase in capacitance in this work can be due to the increased charge carrier density accumulation and changes in relative dielectric permittivity at the interfacial capacitance which have resulted in an increase in capacitance [16, 21]. Changes in capacitance as a result of successive PBS incubations were not as significant as changes in capacitance with LDL incubations. After 6 PBS incubations, with each having an incubation time of 5 min, the change in capacitance was around 50 nF. The results observed here show that the biosensors are sensitive towards LDL. Although, with successive incubations with PBS, the change in capacitance increases almost linearly, the change in capacitance as a result of incubating the biosensor with any LDL-antigen concentration reported here is, at least, 5 times larger than the change in capacitance due to incubating with the blank sample. The increasing change in capacitance due to incubating with PBS can be related to salt concentrations in PBS which affect the interfacial capacitance or other environmental factors such as temperature and humidity [25, 27, 28].

Figure 4b shows the calibration curve of the biosensor. The blue solid line is the linear fitting of the data shown in Fig. 4a (i.e. from 50 pg/mL to 500 ng/mL LDL concentration). The sensitivity of the biosensors, found from the slope of the calibration curve, is 70 nF/log(ng/mL) and the limit of detection (LoD) of the biosensor is 120 pg/mL. LoD was calaculated using Eq. (1) depicted from previous studies [29, 30]:

$$X_{\mathrm{LoD}} = f^{-1}(\bar{y}\mathrm{blank} + 3\sigma) \tag{1}$$

where f^{-1} represents the inverse function of the linear fitting curve in Fig. 4b. $\bar{y}$blank represents the mean value of the readout of the blank sample (PBS) and σ represents the standard deviation of the PBS (or blank) sample. The LoD

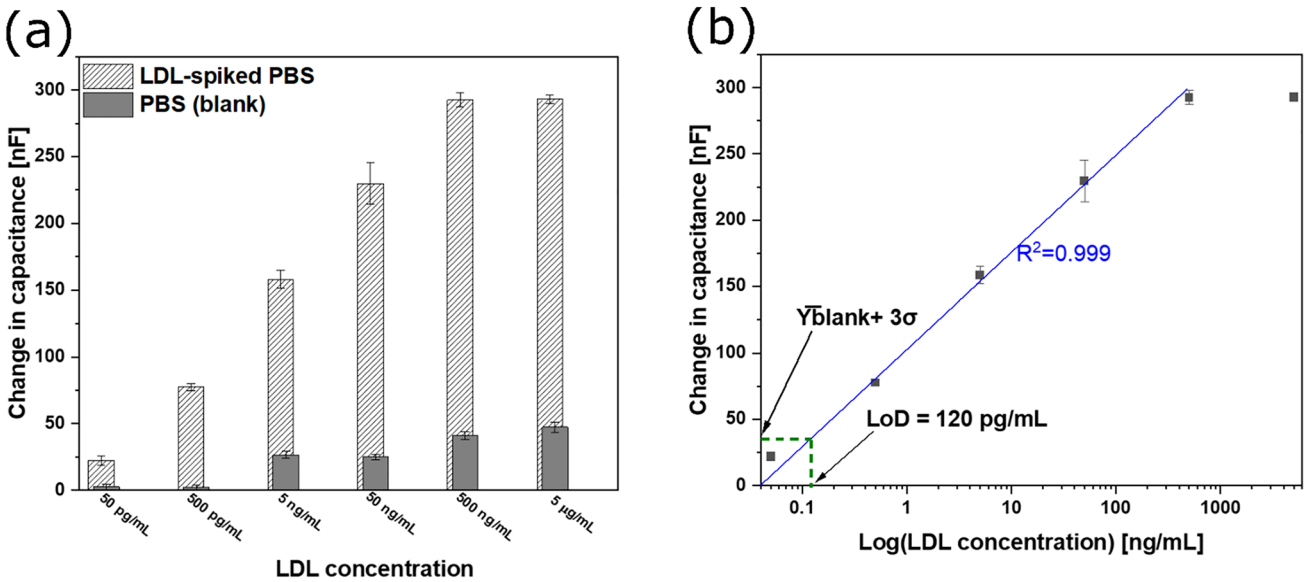

Fig. 4 **a** Average change in capacitance against LDL-spiked PBS and only PBS (blank) samples. **b** Calibration curve of the LDL non-faradaic biosensor

can be found through the intersection between the linear fitting line and $\bar{y}\text{blank} + 3\sigma$ as seen in Fig. 4b. The limit of detection reported here is well below the recommended limit of LDL.

The changes in impedance magnitude (|Z|) and phase at 398 mHz as a result of testing the LDL-antigen with the non-faradaic sensors were also investigated. Figure 5 illustrates the change in |Z| and phase. As can be seen in Fig. 5a and b, as the LDL-antigen concentration increases, |Z| decreases which is expected since both Z_{imag} and Z_{real} represented in Fig. 2 above decreased [31]. A change in impedance of around 45 kΩ and 20 kΩ was observed when testing the sensors against LDL-concentrations and PBS samples, respectively. Furthermore, the change in phase was investigated at 398 mHz (see Fig. 5c and d). As the LDL-antigen concentration increased, the phase increased from 78.47° for the baseline to 81.28° for the highest LDL-antigen concentration (i.e. 5 µg/mL). The average change in phase as a result of testing against PBS samples is 0.69°. Likewise, the LoD was calculated for both |Z| and phase. The LoD for |Z| and phase is 300 pg/mL and 500 pg/mL, respectively. Although the change in phase at 200 mHz is larger than the change in phase at 398 mHz, the LoD at 398 mHz is better than that at 200 mHz. To summarize, the change in capacitance showed a better LoD than the LoD calculated for the change in |Z| and the change in phase.

The selectivity of the biosensors was also investigated in this study. The biosensor was tested against two

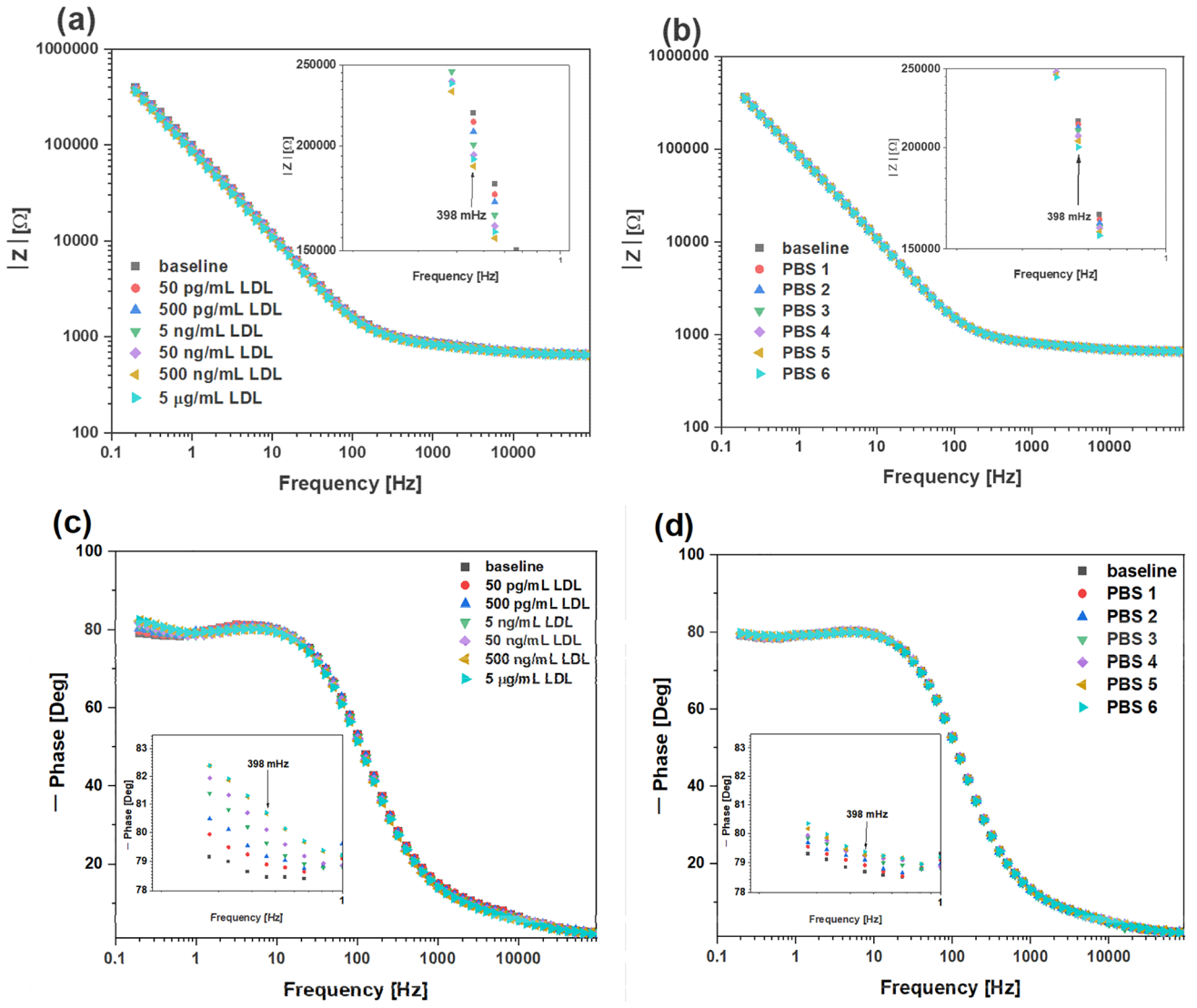

Fig. 5 Bode plot representing |Z| as a result of testing the sensors against **a** different concentrations of LDL-antigen and **b** successive PBS (blank) incubations. Bode plot representing phase when testing the sensors against **a** different concentrations of LDL-antigen and **b** successive PBS (blank) incubations

different samples. One sample consists of LDL-antigen, pepsin, UL83-antigen and *E. coli* (positive sample). The other sample consists of all the antigens except LDL-antigen (negative sample). The concentration of each antigen was 500 pg/mL. Figure 6a and b show typical Bode plots in the frequency range 200 mHz to 1 Hz of the biosensors tested against positive and negative samples, respectively. The resultant change in capacitance at 398 mHz due to incubating the biosensor with the positive sample is around 100 nF, whereas the change in capacitance due to incubating the biosensor with the negative sample is around 25 nF. The results here demonstrate the selectivity of the biosensor towards LDL. More importantly, testing was done against a mixture of proteins, bacteria, viral proteins which mimics real samples testing.

The binding affinity and dissociation constant (K_D) were also investigated. The dissociation constant (K_D) parameter was used to describe the binding affinity between LDL-antibody and LDL-antigen. The smaller the value of K_D the better the binding affinity between the antibody and the antigen. The larger the value of K_D the weaker the affinity between the antibody and the antigen. K_D is expressed using a Langmuir adsorption model-based approach [15, 32, 33]. The equilibrium of the LDL-antigen (M) and LDL antibody (N) can be represented as:

$$(MN) \rightarrow (M) + (N) \tag{2}$$

$$K_D = (M)(N)/(MN) \tag{3}$$

The surface coverage of the LDL-antibody-antigen complex (MN) was adopted as Ø and the surface coverage of the unbound LDL-antibody was 1-Ø; therefore, K_D was determined from:

$$K_D = ((1 - \infty)/\infty)(M) \tag{4}$$

Change in capacitance (ΔC) is assumed from the Langmuir adsorption model and is directly connected to LDL-antibody-antigen binding as:

$$\Delta C = \infty\left(\Delta C_{max}\right) \tag{5}$$

where ΔC_{max} is the maximum biosensor response and equals to $(C_{LDLmax} - C_o)/C_o$. C_{LDLmax} is the maximum capacitance of our biosensor toward LDL-antigen and C_o is the capacitance of the Au-IDEs-anti-LDL biosensor (i.e. baseline capacitance). From Eqs. (4) and (5) a linearized form of the Langmuir-isotherm equation can be written as:

$$(M)/\Delta C = (M)/\Delta C_{max} + K_D/\Delta C_{max} \tag{6}$$

where (M) represents the concentration of LDL-antigen ($Conc_{LDL}$ [pg/mL]). From Eq. (6), a linear regression curve (with a correlation coefficient of 0.96) of $Conc_{LDL}$ against $Conc_{LDL}/\Delta C$ was plotted as seen in Fig. 7. K_D can be obtained by dividing the y-intercept by the slope of the linear. Using this method we obtained a K_D of 4.3 pg/mL which corresponds to 39.09 pM. The dissociation constant (K_D) reported here is smaller than that of other LDL–binding partner interactions, which suggests that the LDL-antibody reported here has a high affinity towards the LDL-antigen and that the reported sensor is suitable for LDL-cholesterol detection [34, 35].

Table 1 shows a comparison of different LDL biosensors. The non-faradaic biosensor reported here shows comparable

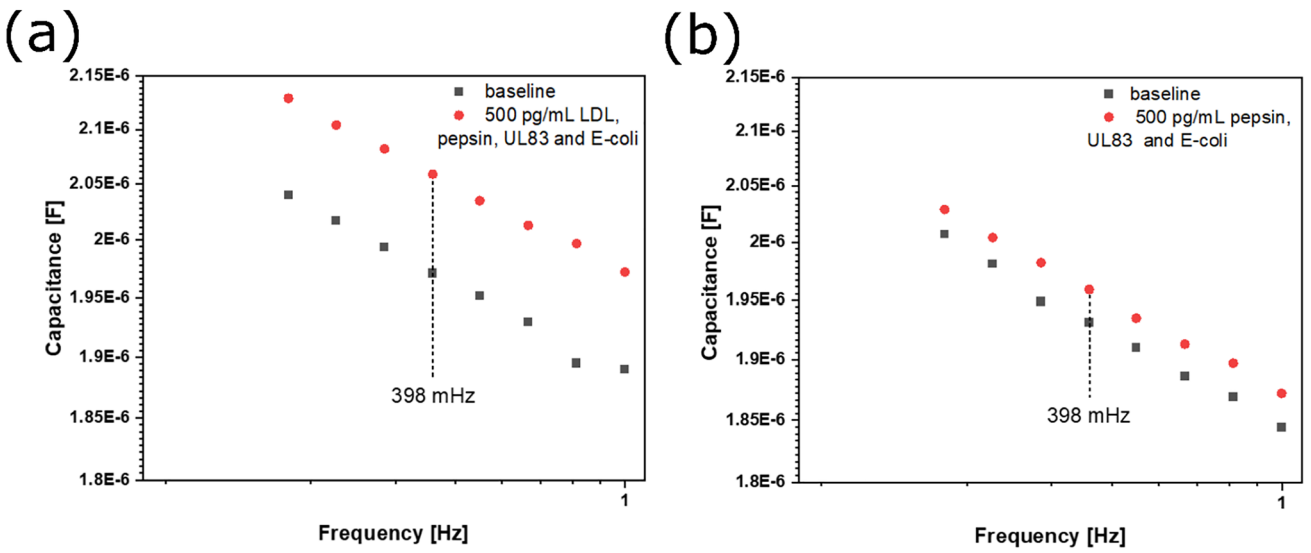

Fig. 6 Selectivity behavior of the biosensors against **a** positive samples (containing LDL-antigen) and **b** negative samples (without LDL-antigen)

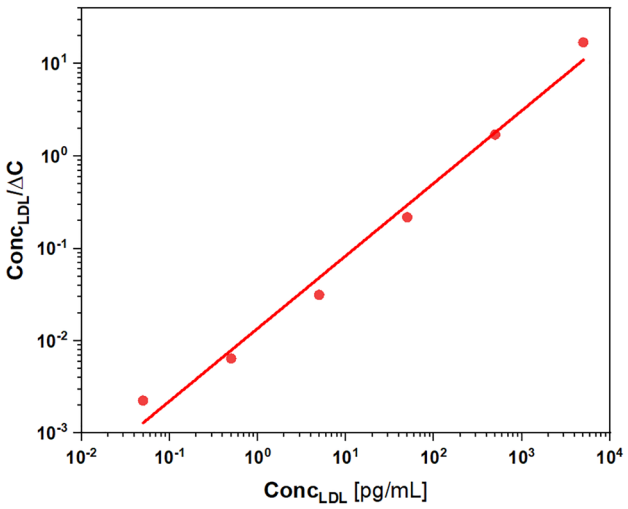

Fig. 7 Plot of $Conc_{LDL}/\Delta C$ fitted with Eq. (6) to determine K_D

and sometimes superior LDL-detection performances. The non-faradaic biosensor reported here is simple and does not require the use of redox mediators or reference electrodes during detection which makes them more desirable for mass production and individual use.

3.2 Continuous Monitoring

In this section, we investigated the ability of the biosensor to continuously monitor the level of LDL in PBS. Such an approach is promising for detecting chronic diseases biomarkers on-site and at intensive care units so that LDL (or other biomarkers) levels can be rapidly measured and early interventions by clinicians can be taken. In this approach, we set the EIS to run at a single frequency (i.e. 398 mHz). Initially, the biosensor was introduced with 50 µL PBS to measure the baseline as seen in Fig. 8 (black solid line). Then, 500 pg/mL LDL was injected into the PBS droplet while the EIS is running (the arrow indicates where the LDL injection was performed). Each EIS cycle lasted for 15 s. The injection of 500 pg/mL LDL resulted in an increase in capacitance of around 50 nF. After 4 EIS cycles (i.e. after 1 min) the biosensor appears to be settled. Then a higher concentration (5 ng/mL) of LDL was injected and resulted in a further increase in capacitance of around 50 nF and the measurement was left to run for 1 min until it settled. Then a higher LDL concentration of 50 ng/mL was added and the capacitance increased by around 50 nF. Again, the EIS measurement was repeated four times until there is no significant change in capacitance. An increase in capacitance of around 50 nF was observed when injecting 500 ng/mL LDL. Further increasing the

Table 1 List of different LDL biosensors

LDL biosensor type	Electrode matrix	Sensitivity	Detection limit	Detection range	References
Electrochemiluminescence	Au/AuNPs/RSH-CdS	–	0.006 ng/mL	0.10–10.34 mmol/L	[36]
Gravimetric	MIP/ZnO NPs	19.285 Hz ng^{-1} mL^{-1}	–	–	[37]
ELISA	N-CDs/Ni-MnFe-LDHs	–	0.0051 mg/dL	0.0625–0.750 mg/dL	[38]
Faradaic EIS	rGO-CdSe QDs/ITO	3.76 md/dL	–	2 mg dL^{-1}–125 mg dL^{-1}	[4]
Protein profiling	AuNPs		0.490 nM	0.05–37.5 µg/mL	[39]
Electrochemiluminescence	Au–Co NPs		0.256 pg mL^{-1}	0.420 to 100 pg mL^{-1}	[40]
Faradaic EIS	Au NPs/β-CDs	978 kΩ μM^{-1}	–	2.5–20 µg/mL	[12]
Square-wave voltammetry (SWV)	Au	–	0.25 ng/mL	0.01 ng/mL to 1.0 ng/mL	[14]
Faradaic EIS	NiO	12 kΩ μM^{-1}	0.015 mM	0.018–0.5 µM	[41]
Faradaic EIS	PANI	11.25 kΩ μM^{-1}	–	018–0.39 µM	[42]
Cyclic voltammetry (CV)	CdS QDs/NiO nanorods	32.08 µA $(mg/dL)^{-1}$ cm^{-2}	0.05 mg/dL	5–120 mg/dL	[13]
Faradaic EIS	ITO/CNT	0.953 Ω/(mg/dL)/cm^2	12.5 mg/dL	0–120 mg/dL	[43]
Faradaic EIS	AuNPs−AgCl@PANI on GCE	–	0.34 pg/mL	–	[44]
QCM	MIP		10 µg/mL	4–400 mg/dL	[45]
SWV	Fe_3O_4@SiO_2	–	0.3 ng/mL	1.0 ng/mL–100 µg/mL	[46]
Faradaic EIS	Au/ CdS QDs	32.8 kΩ μM^{-1}/cm^2	–	5–120 mg/dL	[47]
ELISA assay kit	–	–	0.144 µg/mL	0.312–20 µg/mL	[46]
QCM	Au-NPs/MIP	–	1.5 mg/dL	2.5 mg/dL – 100 mg/ dL	[7]
Optical	Optical fiber	0.0004 mV/ppm	–	–	[48]
Non-faradaic EIS	Au-IDEs	70 nF/log(ng/mL)	120 pg/mL	500 pg/mL – 500 ng/mL	Present work

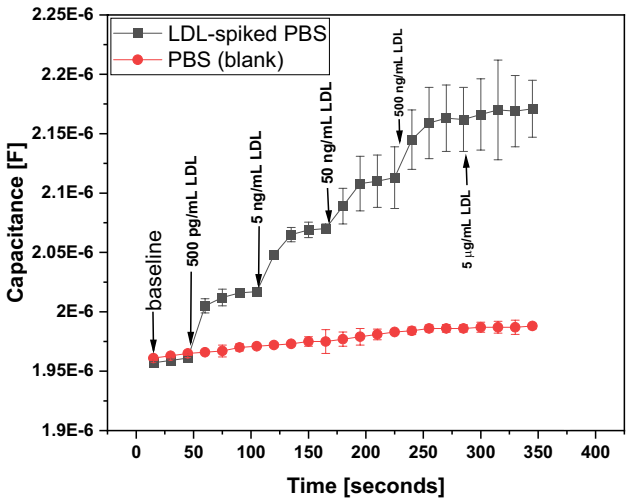

Fig. 8 Continuous monitoring of different LDL concentrations in PBS and against only PBS (blank sample)

LDL concentration (i.e. to 5 µg/mL) resulted in no significant increase in capacitance which suggests that the biosensor saturated after injecting 500 ng/mL LDL. As can be seen, the binding rate of LDL-antigen to LDL-antibody is relatively fast and occurs at an average time of around 1 min. As the LDL concentration increases, the error bar starts to increase which suggests that a few phenomena might have happened at higher concentrations such as agglomeration and steric hindrance. This is due to the fact that rinsing with DI water was not performed after each LDL-antigen injection which have eventually resulted in a large LDL-antigen load at the sensing window and eventually large agglomeration and steric hindrance. The sizes of agglomerations may have interrupted the capture of LDL-antigens by LDL-antibodies. Hence, this resulting in some variations at high LDL concentrations. We also tested our biosensors against PBS (blank samples) to investigate the stability of the biosensors. In this experiment, the sensing window was introduced with 50 µL PBS and EIS measurements were left running for around 350 s. The increase in capacitance is not as significant as the increase in capacitance when injecting LDL concentrations. In addition, there is an increasing shift in capacitance over time. This can be attributed to the content inside the PBS solution being deposited on the biosensor surface over time. This explains the shift in the measured capacitance observed when testing the positive samples. The increase in capacitance due to injecting LDL-concentration is much higher than the increase in capacitance while only testing the negative sample which is very promising. The data reported here is very promising for the development of non-faradaic biosensors for the continuous monitoring of vital biomarkers of chronic diseases on-site and in intensive care units.

4 Conclusion

High cholesterol levels in the blood are a warning sign that the human body is prone to cardiovascular diseases. Current detection techniques are expensive and tedious. In this work, we presented a simple detection method of LDL-cholesterol using non-faradaic impedimetric biosensors. The reported biosensors do not require the use of redox probes or reference electrodes during detection like other electrochemical biosensors. In addition, real-time monitoring of LDL is presented for the first time using the non-faradaic biosensors. The proof of concept presented here is promising for the future development of simple and low-cost devices for the monitoring of dangerous chronic diseases and other diseases.

Acknowledgements The authors would like to acknowledge the support from Taif University Researchers Supporting Project Number (TURSP-2020/264), Taif University, Taif, Saudi Arabia.

Declarations

Conflict of interest The authors declare that they have no known competing financial interests or personal relationships that could have appeared to influence the work reported in this paper.

References

1. Priya, T., Maurya, S.K., Khan, K.H.: Cholesterol: Genet Clinical and Nat Implic. (2013)
2. Sharma, P.K., et al.: Ultrasensitive and reusable graphene oxide-modified double-interdigitated capacitive (DIDC) sensing chip for detecting SARS-CoV-2. ACS Sens. **6**(9), 3468–3476 (2021)
3. Li, L.-H., et al.: Analytical methods for cholesterol quantification. J. Food Drug Anal. **27**(2), 375–386 (2019)
4. Khandelwal, D., et al.: A novel nanocomposite platform of mercaptopropionic acid stabilized CdSe quantum dots-graphene for impedimetric detection of low density lipoprotein. Mater. Lett. **308**, 131236 (2022)
5. Goldstein, J.L., Brown, M.S.: A century of cholesterol and coronaries: from plaques to genes to statins. Cell **161**(1), 161–172 (2015)
6. Grundy, S.M., et al.: Implications of recent clinical trials for the national cholesterol education program adult treatment panel III guidelines. Circulation **110**(2), 227–239 (2004)
7. Chunta, S., et al.: Direct assessment of very-low-density lipoprotein by mass sensitive sensor with molecularly imprinted polymers. Talanta **221**, 121549 (2021)
8. Rahman, M.M., et al.: Photonic crystal fiber based terahertz sensor for cholesterol detection in human blood and liquid foodstuffs. Sens. Bio-Sens. Res. **29**, 100356 (2020)
9. Song, H., et al.: Concentration measurement of LDL cholesterol using extraordinary optical transmission sensor. In: Frontiers in Optics 2015. Optical Society of America, San Jose, California (2015)
10. Raghavan, V., et al.: An enzyme thermistor-based assay for total and free cholesterol. Clin. Chim. Acta. **289**(1–2), 145–158 (1999)

11. Courrol, L.C., et al.: Novel fluorescent probe for low density lipoprotein, based on the enhancement of Europium emission band. Opt. Express **15**(11), 7066–7074 (2007)
12. Wu, H., et al.: Selective molecular recognition of low density lipoprotein based on β-cyclodextrin coated electrochemical biosensor. Biosensors **11**(7), 216 (2021)
13. Ali, M.A., et al.: A biofunctionalized quantum dot–nickel oxide nanorod based smart platform for lipid detection. J. Mat. Chem. B **4**(15), 2706–2714 (2016)
14. Rudewicz-Kowalczyk, D., Grabowska, I.: Detection of low density lipoprotein—comparison of electrochemical immuno- and aptasensor. Sensors **21**(22), 7733 (2021)
15. Le, H.T.N., et al.: Ultrasensitive capacitance sensor to detect amyloid-beta 1–40 in human serum using supramolecular recognition of β-CD/RGO/ITO micro-disk electrode. Talanta **237**, 122907 (2022)
16. Eveness, J., et al.: Equivalent circuit model of a non-faradaic impedimetric ZnO nano-crystal biosensor. J. Electroanal. Chem. **906**, 116003 (2022)
17. Assaifan, A.K., et al.: Label-free and simple detection of trace Pb(II) in tap water using non-faradaic impedimetric sensors. Sens. Actuators A: Phys. **329**, 112833 (2021)
18. Assaifan, A.K., et al.: Nanotextured surface on flexographic printed ZnO thin films for low-cost non-faradaic biosensors. ACS App. Mater. Interfaces **8**(49), 33802–33810 (2016)
19. Wang, L., et al.: Vertically aligned graphene prepared by photonic annealing for ultrasensitive biosensors. ACS App. Mater. Interfaces **12**(31), 35328–35336 (2020)
20. Shanmugam, N.R., Muthukumar, S., Prasad, S.: Ultrasensitive and low-volume point-of-care diagnostics on flexible strips—a study with cardiac troponin biomarkers. Sci. Rep. **6**(1), 33423 (2016)
21. Tanak, A.S., et al.: Non-faradaic electrochemical impedimetric profiling of procalcitonin and C-reactive protein as a dual marker biosensor for early sepsis detection. Anal. Chim. Acta: X **3**, 100029 (2019)
22. Wang, J., et al.: Pepsin in saliva as a diagnostic biomarker in laryngopharyngeal reflux: a meta-analysis. Eur. Arch. Otorhinolaryngol. **275**(3), 671–678 (2018)
23. Saletinger, R., Poljak, M., Strle, F.: Presence of human cytomegalovirus DNA in blood of patients with community-acquired pneumonia. Clin. Microbiol. Infect. **21**(1), 97–102 (2015)
24. Daga, A.P., et al.: *Escherichia coli* bloodstream infections in patients at a University Hospital: virulence factors and clinical characteristics. Front. Cell. Infect. Microbiol. **9**, 191–191 (2019)
25. Daniels, J.S., Pourmand, N.: Label-free impedance biosensors: opportunities and challenges. Electroanalysis **19**(12), 1239–1257 (2007)
26. Bogomolova, A., et al.: Challenges of electrochemical impedance spectroscopy in protein biosensing. Anal. Chem. **81**(10), 3944–3949 (2009)
27. Hassibi, A., Vikalo, H., Hajimiri, A.: On noise processes and limits of performance in biosensors. J. App. Phys. **102**(1), 014909 (2007)
28. Sadik, O.A., et al.: Differential impedance spectroscopy for monitoring protein immobilization and antibody−antigen reactions. Anal. Chem. **74**(13), 3142–3150 (2002)
29. Chiavaioli, F., et al.: Towards a uniform metrological assessment of grating-based optical fiber sensors: from refractometers to biosensors. Biosensors **7**(2), 23 (2017)
30. Cardona-Maya, Y., et al.: Label-free wavelength and phase detection based SMS fiber immunosensors optimized with cladding etching. Sens. Actuators B Chem. **265**, 10–19 (2018)
31. Kinnamon, D., et al.: Portable biosensor for monitoring cortisol in low-volume perspired human sweat. Sci. Rep. **7**(1), 13312 (2017)
32. Huang, Y., Bell, M.C., Suni, I.I.: Impedance biosensor for peanut protein Ara h 1. Anal. Chem. **80**(23), 9157–9161 (2008)
33. Eissa, S., et al.: Selection and identification of DNA aptamers against okadaic acid for biosensing application. Anal. Chem. **85**(24), 11794–11801 (2013)
34. Hodits, R.A., et al.: An antibody fragment from a phage display library competes for ligand binding to the low density lipoprotein receptor family and inhibits rhinovirus infection (∗). J. Biol. Chem. **270**(41), 24078–24085 (1995)
35. Young, S.G., et al.: Conservation of the low density lipoprotein receptor-binding domain of apoprotein B. Demonstration by a new monoclonal antibody, MB47. Arteriosclerosis **6**(2), 178–188 (1986)
36. Jie, G., et al.: CdS nanocrystal-based electrochemiluminescence biosensor for the detection of low-density lipoprotein by increasing sensitivity with gold nanoparticle amplification. Anal. Chem. **79**(15), 5574–5581 (2007)
37. Nasrullah, A., et al.: ZnO nanoparticles and β-cyclodextrin containing molecularly imprinted polymers for gravimetric sensing of very-low-density lipoprotein. Meas. Sci. Technol. **33**(4), 045106 (2022)
38. Prakobkij, A., et al.: Nitrogen-doped carbon dots/Ni-MnFe-layered double hydroxides (N-CDs/Ni-MnFe-LDHs) hybrid nanomaterials as immunoassay label for low-density lipoprotein detection. Microchim. Acta **189**(2), 72 (2022)
39. Cao, J., et al.: Aptamer/AuNPs encoders endow precise identification and discrimination of lipoprotein subclasses. Biosens. Bioelectron. **196**, 113743 (2022)
40. Lian, X., et al.: Direct electrochemiluminescent immunosensing for an early indication of coronary heart disease using dual biomarkers. Anal. Chim. Acta **1110**, 82–89 (2020)
41. Kaur, G., Tomar, M., Gupta, V.: Realization of a label-free electrochemical immunosensor for detection of low density lipoprotein using NiO thin film. Biosens. Bioelectron. **80**, 294–299 (2016)
42. Matharu, Z., et al.: Langmuir-Blodgett films of polyaniline for low density lipoprotein detection. Thin Solid Films **519**(3), 1110–1114 (2010)
43. Ali, M.A., et al.: Chitosan-modified carbon nanotubes-based platform for low-density lipoprotein detection. App. Biochem. Biotechnol. **174**(3), 926–935 (2014)
44. Yan, W., et al.: Fabrication of a label-free electrochemical immunosensor of low-density lipoprotein. J. Phys. Chem. B **112**(4), 1275–1281 (2008)
45. Chunta, S., Suedee, R., Lieberzeit, P.A.: Low-density lipoprotein sensor based on molecularly imprinted polymer. Anal. Chem. **88**(2), 1419–1425 (2016)
46. Wang, J., et al.: A sandwich-type aptasensor for point-of-care measurements of low-density lipoprotein in plasma based on aptamer-modified MOF and magnetic silica composite probes. Microchem. J. **158**, 105288 (2020)
47. Ali, M.A., et al.: Protein-conjugated quantum dots interface: binding kinetics and label-free lipid detection. Anal. Chem. **86**(3), 1710–1718 (2014)
48. Budiyanto, M., Suhariningsih, Yasin, M.: Cholesterol detection using optical fiber sensor based on intensity modulation. J. Phys. Conf. Ser. **853**, 012008 (2017)